Hindawi
Mathematical Problems in Engineering
Volume 2021, Article ID 8427575, 10 pages
https://doi.org/10.1155/2021/8427575

Research Article

Weighted Direct Position Determination via the Dimension Reduction Method for Noncircular Signals

Xinlei Shi [1,2] **and Xiaofei Zhang** [1,2]

[1] *College of Electronic and Information Engineering, Nanjing University of Aeronautics and Astronautics, Nanjing 211106, China*
[2] *Key Laboratory of Dynamic Cognitive System of Electromagnetic Spectrum Space (Nanjing University of Aeronautics and Astronautics), Ministry of Industry and Information Technology, Nanjing 211106, China*

Correspondence should be addressed to Xinlei Shi; 929315571@qq.com

Received 15 August 2021; Accepted 29 November 2021; Published 21 December 2021

Academic Editor: Ruben Specogna

This work studies the direct position determination (DPD) of noncircular (NC) signals with multiple arrays. Existing DPD algorithms of NC sources ignore the impact of path propagation loss on the performance of the algorithms. In practice, the signal-to-noise ratios (SNRs) of different observation stations are often different and unstable when the NC signal of the same radiation target strikes different observation locations. Besides, NC features of the target signals are applied not only to extend the virtual array manifold but also to bring high-dimensional search. For the sake of addressing the above problems, this study develops a DPD method of NC sources for multiple arrays combing weighted subspace data fusion (SDF) and dimension reduction (RD) search. First, NC features of the target signals are applied to extend the virtual array manifold. Second, we assign a weight to balance the error and obtain higher location accuracy with better robustness. Then, the RD method is used to eliminate the high computational complexity caused by the NC phase search dimension. Finally, the weighted fusion cost function is constructed by using the eigenvalues of the received signal covariance matrixes. It is verified by simulation that the proposed algorithm can effectively improve the location performance, get better robustness, and distinguish more targets compared with two-step location technology and SDF technology. In addition, without losing the estimation performance, the proposed algorithm can significantly reduce the complexity caused by the NC phase search dimension.

1. Introduction

As we all know, wireless position determination is a significant research work about signal processing, which has developed rapidly in recent years. It has been widely used in many fields including communication, radar, military, astronomy, and so on [1–4]. Research on wireless location can be divided into two categories: traditional two-step location technology and direct position determination technology (DPD). Traditional two-step location technology: this kind of technology first needs to extract the intermediate parameters including the target position information from the original data, such as direction of arrival. Then, target positions can be calculated from the spatial geometric relationship [5–7]. DPD can directly estimate target positions from the original data without estimating intermediate parameters [8–10].

Theoretically, DPD avoids the transmission of intermediate parameter error and can obtain more accurate estimation results than two-step location technology, so it has been widely concerned. In the modern communication system, according to whether the ellipse covariance is zero or not, the signal could be split into circular signal and noncircular signals [11]. To date, DPD for circular signal has achieved many research results. Weiss proposed a DPD method based on maximum likelihood (ML) in 2007 [12]. Then, Oispuu proposed a DPD technology combining maximum likelihood and Capon in 2010 to improve the estimation accuracy [9]. A DPD method based on time-varying delay is developed by Shangyu, which can effectively

improve the location performance [13]. T Zhou proposed an iterative adaptive DPD method, which can deal with the case of coherent sources [14]. In modern communication systems, quadrature phase shift keying (QPSK) signals and amplitude modulation (AM) signals all belong to NC signals, so it is of great significance for the research of the DPD algorithm with NC sources. However, so far, there are a few research studies on DPD methods for NC signals. The features of NC signals are applied to ameliorate the location accuracy in [15–17]. Then, Doppler shifts have been applied to extend the array manifold for higher estimation accuracy [18, 19]. Recently, the sparse array and spatial smoothing method have been used to realize the DPD of underdetermined conditions [20], [21].

However, the existing methods do not solve the high complexity problem caused by noncircular phase. In addition, the existing DPD methods of NC sources have not considered the impact of path propagation loss, so performances of the relevant algorithms are unstable and the location accuracy has some limitations [22–25]. According to the principle of power allocation in reference [26], combined with the idea of SDF and NC characteristics, this study derives the weighted SDF algorithm for NC sources (NC-WSDF). Due to the high-dimensional search caused by NC phase, this study introduces the idea of dimension reduction search [27, 28] and develops a DPD technology of NC signals with multiple arrays by weighted the SDF and RD method (NRD-WSDF). It is verified by simulation that the proposed method is more robust and has better location performance compared with the traditional two-step technology, SDF technology, and NC-SDF technology. Besides, the proposed DPD technology significantly reduces the computational complexity through the RD method without losing the estimation performance.

The main contributions are summarized as follows:

(1) When the NC signal of the same radiation target strikes different observation locations, the SNRs of different observation stations are often different and unstable because of the path propagation loss. Therefore, a method based on SNR weighting is applied to balance the error and obtain higher location accuracy and higher level of robustness.

(2) Combined with the idea of expanding virtual array aperture based on NC characteristics and SDF algorithm, the NC-WSDF algorithm is derived, which has more degrees of freedom and can distinguish more targets

(3) The RD method is introduced to reduce the high computational complexity caused by NC phase search, and an NRD-WSDF algorithm is proposed, which effectively reduces the computational complexity without losing the estimation performance.

(4) Complexity analysis and simulation results are explained to prove the excellent performance of the proposed algorithm

The rest of the study is given as follows: Section 2 introduces the DPD model with multiple arrays and NC sources model. In Section 3, we develop a DPD method of NC sources for multiple arrays combing weighted subspace data fusion (SDF) and dimension reduction (RD) search. Sections 4 and 5 give the performance analysis and conclusions, respectively.

In this study, vector and matrix are lower-case bold and upper-case bold, respectively; $\|\cdot\|$ represents the l_2 norm; $(\cdot)^*$, $(\cdot)^T$, $(\cdot)^H$, and $(\cdot)^{-1}$ represent conjugate, transposition, conjugate transpose, and the inverse of matrix, respectively; $\mathbf{0}_N$ denotes the N dimensional zero array; $\mathbf{I}_N$ denotes the N dimensional unit array; diag{·} represents the diagonal matrix.

2. Model Formulation

2.1. DPD Model with Multiple Arrays. Consider a two-dimensional localization scene as shown in Figure 1. Suppose that there are K uncorrelated narrow-band noncircular signals incident on L base stations in the far-field, each base station is outfitted with a uniform linear array (ULA), and the interval between arrays is $\lambda/2$, where λ denotes the wavelength. The target positions are $\mathbf{p}_k = [x_k, y_k]^T$ $(k = 1, 2, \ldots, K)$. The locations of the observation stations are $\mathbf{u}_l = [x_l, y_l]^T$ $(l = 1, 2, \ldots, L)$. The number of snapshots per observation station is T.

On the basis of the free space propagation loss model [29–31], the SNRs of different observation stations are different when the signal of the same radiation target strikes different observation locations. The path propagation loss coefficient can be stated as

$$\alpha_{l,k} = \sqrt{\frac{P_{l,k}}{P_k}}, \tag{1}$$

where P_k represents the power of the emitter signal, and $P_{l,k}$ stands for the power of the signal from the k^{th} target received at the l^{th} base location.

Suppose the t^{th} snapshot for the k^{th} target at the l^{th} observation station is $s_{l,k}(t)$. The signal at the t^{th} snapshot received by the l^{th} observation station can be stated as [31]

$$\mathbf{r}_l(t) = \sum_{k=1}^{K} \alpha_{l,k}\mathbf{a}\left(\theta_{l,k}\right)s_{l,k}(t) + \mathbf{n}_l(t), \tag{2}$$

where the steering vector is

$$\mathbf{a}\left(\theta_{l,k}\right) = \left[1, e^{-j\pi\cos\theta_{l,k}}, \ldots, e^{-j\pi(M-1)\cos\theta_{l,k}}\right]^T \in \mathbb{C}^{M\times 1}, \tag{3}$$

where $\theta_{l,k}$ represents azimuth of the k^{th} target received by the l^{th} observation station, and $\mathbf{n}_l(t)$ denotes the Gaussian white noise vector. As the targets are far from the observation stations, the observation stations can be considered as points. Therefore, equation (3) can be stated as

$$\mathbf{a}_l\left(\mathbf{p}_k\right) = \left[1, \ldots, e^{-j\pi(M-1)\left(\mathbf{u}_l(1)-\mathbf{p}_k(1)/\|\mathbf{u}_l-\mathbf{p}_k\|\right)}\right]^T \in \mathbb{C}^{M\times 1}, \tag{4}$$

where $||\cdot||$ represents the l_2 norm.

Thus, equation (2) can be simplified as

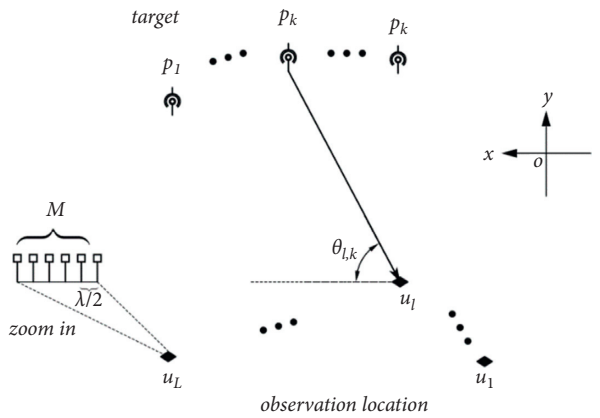

Figure 1: Geometry of multiple arrays.

$$\mathbf{r}_l(t) = \mathbf{A}_l(\mathbf{p})\mathbf{\Lambda}\mathbf{s}_l(t) + \mathbf{n}_l(t) \in \mathbb{C}^{M\times 1}, \tag{5}$$

where

$$\begin{aligned}
\mathbf{A}_l(\mathbf{p}) &= \left[\mathbf{a}_l(\mathbf{p}_1), \mathbf{a}_l(\mathbf{p}_2), \ldots, \mathbf{a}_l(\mathbf{p}_K)\right] \in \mathbb{C}^{M\times K},\\
\mathbf{\Lambda} &= \begin{bmatrix} \alpha_{l,1} & 0 & \ldots & 0 \\ 0 & \alpha_{l,2} & \ddots & \vdots \\ \vdots & \ddots & \ddots & 0 \\ 0 & \ldots & 0 & \alpha_{l,K} \end{bmatrix} \in \mathbb{R}^{K\times K},\\
\mathbf{s}_l(t) &= \left[s_{l,1}(t), \ldots, s_{l,K}(t)\right]^T \in \mathbb{C}^{K\times 1},\\
\mathbf{p} &= \left[\mathbf{p}_1^T, \mathbf{p}_2^T, \ldots, \mathbf{p}_K^T\right]^T,\\
\mathbf{n}_l(t) &= \left[\mathbf{n}_{l,1}(t), \mathbf{n}_{l,2}(t), \ldots, \mathbf{n}_{l,M}(t)\right]^T \in \mathbb{C}^{M\times 1},
\end{aligned} \tag{6}$$

where $(\cdot)^T$ denotes the transposition.

2.2. Noncircular Sources Model. According to [11], we can get the following equation:

$$E\left[\mathbf{s}_l(t)\mathbf{s}_l^H(t)\right] = \rho e^{j\varphi} E\left[\mathbf{s}_l(t)\mathbf{s}_l^T(t)\right], \tag{7}$$

where φ represents the noncircular phase, $\rho(\rho \in [0,1])$ denotes the noncircular ratio, and $(\cdot)^H$ stands for the conjugate transpose. For the sake of simplicity, this study only considers the case that the noncircular ratio is 1. From [15], NC signals can be written as

$$\mathbf{s}_l(t) = \mathbf{\Phi}\mathbf{s}_l^{(R)}(t), \tag{8}$$

where

$$\begin{aligned}
\mathbf{\Phi} &= \begin{bmatrix} e^{-j\varphi_1} & 0 & \ldots & 0 \\ 0 & e^{-j\varphi_2} & \ddots & \vdots \\ \vdots & \ddots & \ddots & 0 \\ 0 & \ldots & & e^{-j\varphi_K} \end{bmatrix} \in \mathbb{C}^{K\times K},\\
\mathbf{s}_l^{(R)}(t) &= \left[s_{l,1}^{(R)}(t), s_{l,2}^{(R)}(t), \ldots, s_{l,K}^{(R)}(t)\right]^T \in \mathbb{R}^{K\times 1},
\end{aligned} \tag{9}$$

where φ_k stands for the NC phase of the k^{th} signal, and $s_{l,k}^{(R)}(t)$ denotes the signal amplitude.

3. The Proposed Algorithm

3.1. NC-WSDF. According to equation (8), equation (5) can be rewritten as

$$\mathbf{r}_l(t) = \mathbf{A}_l(\mathbf{p})\mathbf{\Lambda}\mathbf{\Phi}\mathbf{s}_l^{(R)}(t) + \mathbf{n}_l(t) \in \mathbb{C}^{M\times 1}. \tag{10}$$

On the basis of the noncircular characteristics in [21], the received signal vector can be extended to

$$\mathbf{z}_l(t) = \begin{bmatrix} \mathbf{r}_l(t) \\ \mathbf{r}_l^*(t) \end{bmatrix} = \begin{bmatrix} \mathbf{A}_l(t)\mathbf{\Lambda}\mathbf{s}_l(t) \\ \mathbf{A}_l^*(t)\mathbf{\Lambda}^*\mathbf{s}_l^*(t) \end{bmatrix} + \begin{bmatrix} \mathbf{n}_l(t) \\ \mathbf{n}_l^*(t) \end{bmatrix} \in \mathbb{C}^{2M\times 1}, \tag{11}$$

where $(\cdot)^*$ denotes the conjugate.

As

$$\mathbf{s}_l^*(t) = \mathbf{\Phi}^*\mathbf{s}_l^{(R)*}(t) = \mathbf{\Phi}^*\mathbf{\Phi}^{-1}\mathbf{s}_l(t) = \left(\mathbf{\Phi}^*\right)^2\mathbf{s}_l(t), \tag{12}$$

where $(\cdot)^{-1}$ stands for the inverse of matrix.

Thus, equation (11) can be expressed as

$$\begin{aligned}
\mathbf{z}_l(t) &= \begin{bmatrix} \mathbf{A}_l(t) \\ \mathbf{A}_l^*(t)\mathbf{\Phi}^*\mathbf{\Phi}^* \end{bmatrix}\mathbf{\Lambda}\mathbf{s}_l(t) + \begin{bmatrix} \mathbf{n}_l(t) \\ \mathbf{n}_l^*(t) \end{bmatrix}\\
&= \mathbf{B}_l(\mathbf{p})\mathbf{\Lambda}\mathbf{s}_l(t) + \begin{bmatrix} \mathbf{n}_l(t) \\ \mathbf{n}_l^*(t) \end{bmatrix} \in \mathbb{C}^{2M\times 1},
\end{aligned} \tag{13}$$

where

$$\begin{aligned}
\mathbf{B}_l(\mathbf{p}) &= \begin{bmatrix} \mathbf{A}_l(t) \\ \mathbf{A}_l^*(t)\mathbf{\Phi}^*\mathbf{\Phi}^* \end{bmatrix}\\
&= \left[\mathbf{b}_l(\mathbf{p}_1, \varphi_1), \mathbf{b}_l(\mathbf{p}_2, \varphi_2), \ldots, \mathbf{b}_l(\mathbf{p}_K, \varphi_K)\right] \in \mathbb{C}^{2M\times K},\\
\mathbf{b}_l(\mathbf{p}_k, \varphi_k) &= \begin{bmatrix} \mathbf{a}_l(\mathbf{p}_k) \\ \mathbf{a}_l^*(\mathbf{p}_k)e^{-j2\varphi_k} \end{bmatrix} \in \mathbb{C}^{2M\times 1}.
\end{aligned} \tag{14}$$

Then, we can get the covariance matrix of signals received by the l^{th} observation location:

$$\mathbf{R}_l = \frac{1}{T}\sum_{t=1}^{T}\mathbf{z}_l(t)\mathbf{z}_l^H(t). \tag{15}$$

The eigenvalue decomposition (EVD) of $\mathbf{R}_l$ is carried out [28].

$$\mathbf{R}_l = \left[\mathbf{U}_l^{(s)}, \mathbf{U}_l^{(n)}\right]\mathbf{\Sigma}_l\left[\mathbf{U}_l^{(s)}, \mathbf{U}_l^{(n)}\right]^H. \tag{16}$$

If we use $\lambda_{l,m}(m = 1, 2, \ldots, 2M)$ to represent the eigenvalues of the l^{th} observation location, which is sorted from large to small, the corresponding eigenvectors are represented by $\mathbf{e}_{l,m}(m = 1, 2, \ldots, 2M)$. Then, in equation (16), signal subspace and noise subspace can be expressed as $\mathbf{U}_l^s = [\mathbf{e}_{l,1}, \ldots, \mathbf{e}_{l,K}]$ and $\mathbf{U}_l^n = [\mathbf{e}_{l,K+1}, \ldots, \mathbf{e}_{l,2M}]$, respectively, and $\Sigma_l = \text{diag}\{\lambda_{l,1}, \lambda_{l,2}, \ldots, \lambda_{l,2M}\}$, where diag{·} represents the diagonal matrix.

Then, we can get the cost function according to the idea of

$$\mathbf{f}_{NC-SDF}(\mathbf{p},\boldsymbol{\varphi}) = \arg\min_{\mathbf{p},\boldsymbol{\varphi}} \sum_{l=1}^{L} \left\| \left(\mathbf{U}_l^{(n)}\right)^H \mathbf{b}_l(\mathbf{p},\boldsymbol{\varphi}) \right\|^2. \quad (17)$$

However, the cost function in equation (17) does not consider the influence of path propagation loss matrix Λ. In practice, the path propagation loss cannot be ignored [29]. As long as there is one with poor performance, the cost function is easily disturbed. Therefore, in order to balance the projection error, obtain higher location accuracy and higher level of robustness, and we assign weight as

$$\mathbf{f}_{\mathrm{NC-WSDF}}(\mathbf{p},\boldsymbol{\varphi}) = \arg\min_{\mathbf{p},\boldsymbol{\varphi}} \sum_{l=1}^{L} \mathbf{w}_l \left\| \left(\mathbf{U}_l^{(n)}\right)^H \mathbf{b}_l(\mathbf{p},\boldsymbol{\varphi}) \right\|^2, \quad (18)$$

where $\mathbf{w}_l$ is the weight of the l^{th} observation station.

As higher SNR will lead to smaller error, we can use SNR to weight the projection result of each observation location. Therefore, we rewrite equation (15) by substituting equation (13) into equation (15):

$$\mathbf{R}_l = \frac{1}{T}\sum_{t=1}^{T}\left[\sum_{k=1}^{K} \alpha_{l,k}^2 \mathrm{P}_k \mathbf{b}_l(\mathbf{p},\boldsymbol{\varphi})\mathbf{b}_l^H(\mathbf{p},\boldsymbol{\varphi}) + \sigma_n^2 \mathbf{I}_{2M\times 2M}\right], \quad (19)$$

where $\mathbf{I}_N$ denotes the N dimensional unit array.

Under the assumption that the noise power is stationary during the observation, it can be seen from equation (19) that the SNR of different base stations is proportional to $\alpha_{l,k}^2 P_k$, i.e., $P_{l,k}$, which is unknown in practice. However, the covariance matrix can be decomposed into SDH:

$$\begin{aligned}\mathbf{R}_l &= \mathbf{R}_s + \mathbf{R}_n = \mathbf{B}_l(\mathbf{p},\boldsymbol{\varphi})\mathrm{diag}\left\{\mathrm{P}_{l,1},\ldots,\mathrm{P}_{l,K}\right\}\mathbf{B}_l^H(\mathbf{p},\boldsymbol{\varphi}) \\ &\quad + \sigma_{n,l}^2 \mathbf{I}_{2M\times 2M}.\end{aligned} \quad (20)$$

Under the same assumption, the eigenvalues of covariance matrix can be expressed as

$$\lambda_{l,m} = \begin{cases} \sigma_{s,m}^2 + \sigma_{n,l}^2, & 1 \le m \le K, \\ \sigma_{n,l}^2, & K+1 \le m \le 2M, \end{cases} \quad (21)$$

where $\sigma_{s,m}^2 (1 \le m \le K)$ are the larger nonzero eigenvalues of $\mathbf{R}_s$, which represent the power of the received signal. Then, the noise power can be expressed as

$$\widehat{\sigma}_{n,l}^2 = \frac{1}{2M-K}\sum_{m=K+1}^{2M} \lambda_{l,m}. \quad (22)$$

According to the estimated noise power, the estimated signal power of the l^{th} observation location can be obtained as follows:

$$\widehat{\mathrm{P}}_l = \sum_{m=K+1}^{2M} \left(\lambda_{l,m} - \widehat{\sigma}_{n,l}^2\right). \quad (23)$$

Then, we can get the weighted cost function:

$$\mathbf{f}_{\mathrm{NC-WSDF}}(\mathbf{p},\boldsymbol{\varphi}) = \arg\min_{\mathbf{p},\boldsymbol{\varphi}} \sum_{l=1}^{L} \frac{\widehat{\mathrm{P}}_l}{\widehat{\sigma}_{n,l}^2} \left\| \left(\mathbf{U}_l^{(n)}\right)^H \mathbf{b}_l(\mathbf{p},\boldsymbol{\varphi}) \right\|^2. \quad (24)$$

3.2. NRD-WSDF. To reduce the complexity and improve the practicability of the algorithm, the idea of dimension reduction in [32] and [33] is introduced to remove the noncircular phase search dimension. Since $\mathbf{s}_l^{(R)}(t)$ is a real vector, we can get

$$\mathbf{s}_l^{(R)}(t) = \mathbf{s}_l^{(R)*}(t). \quad (25)$$

Thus, equation (11) can be rewritten as

$$\begin{aligned}\mathbf{z}_l(t) &= \begin{bmatrix} \mathbf{r}_l(t) \\ \mathbf{r}_l^*(t) \end{bmatrix} = \begin{bmatrix} \mathbf{A}_l(t)\boldsymbol{\Phi} \\ \mathbf{A}_l^*(t)\boldsymbol{\Phi}^* \end{bmatrix}\boldsymbol{\Lambda}\mathbf{s}_l(t) + \begin{bmatrix} \mathbf{n}_l(t) \\ \mathbf{n}_l^*(t) \end{bmatrix} \\ &= \mathbf{H}_l(\mathbf{p},\boldsymbol{\varphi})\boldsymbol{\Lambda}\mathbf{s}_l(t) + \mathbf{n}_l^c(t),\end{aligned} \quad (26)$$

where

$$\begin{aligned}\mathbf{H}_l(\mathbf{p},\boldsymbol{\varphi}) &= \begin{bmatrix} \mathbf{A}_l(t)\boldsymbol{\Phi} \\ \mathbf{A}_l^*(t)\boldsymbol{\Phi}^* \end{bmatrix} \\ &= \left[\mathbf{h}_l(\mathbf{p}_1,\boldsymbol{\varphi}_1),\ldots,\mathbf{h}_l(\mathbf{p}_K,\boldsymbol{\varphi}_K)\right] \in \mathbb{C}^{2M\times K},\end{aligned} \quad (27)$$

$$\mathbf{n}_l^c(t) = \begin{bmatrix} \mathbf{n}_l(t) \\ \mathbf{n}_l^*(t) \end{bmatrix} \in \mathbb{C}^{2M\times 1}, \quad (28)$$

$$\mathbf{h}_l(\mathbf{p}_k,\boldsymbol{\varphi}_k) = \begin{bmatrix} \mathbf{a}_l(\mathbf{p}_k)e^{-j\boldsymbol{\varphi}_k} \\ \mathbf{a}_l^*(\mathbf{p}_k)e^{j\boldsymbol{\varphi}_k} \end{bmatrix} \in \mathbb{C}^{2M\times 1}. \quad (29)$$

Equation (29) is an extended steering vector, which contains the position information and noncircular phase information of the k^{th} target. In order to separate the position information from the noncircular phase information, matrix conversion is performed as

$$\begin{aligned}\mathbf{h}_l(\mathbf{p}_k,\boldsymbol{\varphi}_k) &= \begin{bmatrix} \mathbf{a}_l(\mathbf{p}_k)e^{-j\boldsymbol{\varphi}_k} \\ \mathbf{a}_l^*(\mathbf{p}_k)e^{j\boldsymbol{\varphi}_k} \end{bmatrix} = \begin{bmatrix} \mathbf{a}_l(\mathbf{p}_k) & \mathbf{0}_{M\times 1} \\ \mathbf{0}_{M\times 1} & \mathbf{a}_l^*(\mathbf{p}_k) \end{bmatrix}\begin{bmatrix} e^{-j\boldsymbol{\varphi}_k} \\ e^{j\boldsymbol{\varphi}_k} \end{bmatrix} \\ &= \mathbf{C}(\mathbf{p}_k)\boldsymbol{\eta}(\boldsymbol{\varphi}_k),\end{aligned} \quad (30)$$

where $\mathbf{0}_N$ denotes the N dimensional zero array.

$$\begin{aligned}\mathbf{C}(\mathbf{p}_k) &= \begin{bmatrix} \mathbf{a}_l(\mathbf{p}_k) & \mathbf{0}_{M\times 1} \\ \mathbf{0}_{M\times 1} & \mathbf{a}_l^*(\mathbf{p}_k) \end{bmatrix}, \\ \boldsymbol{\eta}(\boldsymbol{\varphi}_k) &= \begin{bmatrix} e^{-j\boldsymbol{\varphi}_k} \\ e^{j\boldsymbol{\varphi}_k} \end{bmatrix}.\end{aligned} \quad (31)$$

Then, we can get the loss function of the l^{th} observation location:

$$\mathbf{f}_l(\mathbf{p},\boldsymbol{\varphi}) = \arg\min_{\mathbf{p},\boldsymbol{\varphi}} \frac{\widehat{\mathrm{P}}_l}{\widehat{\sigma}_{n,l}^2}\boldsymbol{\eta}^H(\boldsymbol{\varphi})\mathbf{J}_l(\mathbf{p})\boldsymbol{\eta}(\boldsymbol{\varphi}). \quad (32)$$

It is obvious that

$$\begin{aligned}\mathbf{f}_l(\mathbf{p},\boldsymbol{\varphi}) &= e^{-j\boldsymbol{\varphi}}\mathbf{f}_l(\mathbf{p},\boldsymbol{\varphi})e^{j\boldsymbol{\varphi}},\\ &= \arg\min_{\mathbf{p},\boldsymbol{\varphi}} e^{-j\boldsymbol{\varphi}}\frac{\widehat{\mathrm{P}}_l}{\widehat{\sigma}_{n,l}^2}\boldsymbol{\eta}^H(\boldsymbol{\varphi})\mathbf{J}_l(\mathbf{p})\boldsymbol{\eta}(\boldsymbol{\varphi})e^{j\boldsymbol{\varphi}}\\ &= \arg\min_{\mathbf{p},\boldsymbol{\varphi}} \frac{\widehat{\mathrm{P}}_l}{\widehat{\sigma}_{n,l}^2}\mathbf{g}^H(\boldsymbol{\varphi})\mathbf{J}_l(\mathbf{p})\mathbf{g}(\boldsymbol{\varphi}),\end{aligned} \tag{33}$$

where

$$\begin{aligned}\mathbf{g}^H(\boldsymbol{\varphi}) &= \boldsymbol{\eta}(\boldsymbol{\varphi})e^{j\boldsymbol{\varphi}} = \begin{bmatrix}1\\ e^{j2\boldsymbol{\varphi}}\end{bmatrix},\\ \mathbf{J}_l(\mathbf{p}) &= \mathbf{C}^H(\mathbf{p})\mathbf{U}_l^{(n)}\left(\mathbf{U}_l^{(n)}\right)^H\mathbf{C}(\mathbf{p}).\end{aligned} \tag{34}$$

Equation (33) is a quadratic optimization problem for unknown parameter φ. Thus, we can reconstruct the optimization problem as [28]

$$\begin{aligned}&\min_{\mathbf{p},\boldsymbol{\varphi}} \mathbf{g}^H(\boldsymbol{\varphi})\mathbf{J}_l(\mathbf{p})\mathbf{g}(\boldsymbol{\varphi}),\\ &\text{s.t.}\quad \overline{\eta}^H\mathbf{g}(\boldsymbol{\varphi}) = 1,\end{aligned} \tag{35}$$

where

$$\overline{\eta} = \begin{bmatrix}1\\ 0\end{bmatrix}. \tag{36}$$

In order to solve the above optimization problem, the Lagrange method is adopted, so the following functions are constructed:

$$\mathbf{L}(\mathbf{p},\boldsymbol{\varphi}) = \mathbf{g}^H(\boldsymbol{\varphi})\mathbf{J}_l(\mathbf{p})\mathbf{g}(\boldsymbol{\varphi}) - \mu\left[\overline{\eta}^H\mathbf{g}(\boldsymbol{\varphi}) - 1\right], \tag{37}$$

where μ in equation (37) is the Lagrange multiplier. Let the derivative of $\mathbf{L}(\mathbf{p},\varphi)$ over $\eta(\varphi)$ be zero.

$$\frac{\partial\mathbf{L}(\mathbf{p},\boldsymbol{\varphi})}{\partial\boldsymbol{\eta}(\boldsymbol{\varphi})} = 2\mathbf{J}_l(\mathbf{p})\mathbf{g}(\boldsymbol{\varphi}) + \mu\overline{\eta} = 0. \tag{38}$$

Then, we can get

$$\mathbf{g}(\boldsymbol{\varphi}) = \kappa\mathbf{J}_l(\mathbf{p})^{-1}\overline{\eta}. \tag{39}$$

Since $\overline{\eta}^H\mathbf{g}(\varphi) = 1$,

$$\begin{aligned}\kappa &= \frac{1}{\overline{\eta}^H\mathbf{J}_l(\mathbf{p})^{-1}\overline{\eta}},\\ \mathbf{g}(\boldsymbol{\varphi}) &= \frac{\mathbf{J}_l(\mathbf{p})^{-1}\overline{\eta}}{\overline{\eta}^H\mathbf{J}_l(\mathbf{p})^{-1}\overline{\eta}}.\end{aligned} \tag{40}$$

Thus, equation (32) can be reduced to

$$\mathbf{f}_l(\mathbf{p}) = \arg\min_{\mathbf{p}} \frac{\widehat{\mathrm{P}}_l}{\widehat{\sigma}_{n,l}^2}\frac{1}{\overline{\eta}^H\mathbf{J}_l(\mathbf{p})^{-1}\overline{\eta}}. \tag{41}$$

Finally, we can get the cost function of NRD-WSDF:

$$\mathbf{f}_{\mathrm{NRD-WSDF}}(\mathbf{p}) = \min_{\mathbf{p}}\sum_{l=1}^{L}\left[\frac{\widehat{\mathrm{P}}_l}{\widehat{\sigma}_{n,l}^2}\frac{1}{\overline{\eta}^H\left(\mathbf{C}^H(\mathbf{p})\mathbf{U}_l^{(n)}\left(\mathbf{U}_l^{(n)}\right)^H\mathbf{C}(\mathbf{p})\right)^{-1}\overline{\eta}}\right]. \tag{42}$$

Through spectral peak search, the K minimum points correspond to the target positions.

3.3. Main Steps of the Proposed Algorithm. The main steps of NRD-WSDF are summarized as follows:

1. Construct the NC-DPD model according to equation (10)
2. Expand the received signal vector according to equation (11) and calculate the covariance matrix $\mathbf{R}_l$ considering equation (15). Then, we can obtain the noise subspace $\mathbf{U}_l^{(n)}$ by equation (16).
3. Get $\widehat{\sigma}_{n,l}^2$ and $\widehat{\mathrm{P}}_l$ from equation (22) and equation (23)
4. Use equation (36) and equation (42) to get $\mathbf{f}_{NRD-WSDF}(\mathbf{p})$
5. Through spectral peak search, the K minimum points correspond to the target positions

3.4. Summary of Algorithm Advantages. Advantages of NRD-WSDF are as follows.

(1) The estimation accuracy and the robustness of the proposed NRD-WSDF algorithm are better than that of two-step location technology, SDF technology, and NC-SDF method

(2) The proposed NRD-WSDF method has more degrees of freedom and can distinguish more targets compared with the two-step location technology and SDF algorithm

(3) The proposed NRD-WSDF algorithm can significantly reduce the complexity caused by the NC phase without losing the estimation performance

4. Performance Analysis

4.1. Complexity Analysis. The complexity of the algorithms is analyzed as follows: the number of array elements is M, the number of targets is K, and the number of snapshots is T. L represents the number of observation stations. L_x, L_y, L_θ, and L_φ stand for the number of search grids of x coordinates, y coordinates, angles, and NC phase. The NC-WSDF algorithm in this study is mainly composed of three steps: the calculation of covariance matrix, EVD, and the calculation of searching spectral function. The corresponding computational complexity is $4LTM^2$, $8LM^3$, and $LL_xL_yL_\varphi[8M^3 - 4M^2K + 4M^2 + 2M]$. In contrast, the complexity of spectral function search for the proposed NRD-WSDF algorithm is $LL_xL_y[8M^3 - 4M^2K + 8M^2 + 8M + 14]$, which

Table 1: Complexity of different algorithms.

Algorithm	Complexity
Two-step	$O(LM^3 + (LT + L_\theta)M^2 - L_\theta KM + LKL_xL_y)$
SDF	$O(LTM^2 + LM^3 + LL_xL_y(M^2(M-K) + M^2 + M))$
NC-SDF	$O(4LTM^2 + 8LM^3 + LL_xL_yL_\varphi(8M^3 - 4M^2K + 4M^2 + 2M))$
NC-WSDF	$O(4LTM^2 + 8LM^3 + LL_xL_yL_\varphi(8M^3 - 4M^2K + 4M^2 + 2M))$
NRD-WSDF	$O(4LTM^2 + 8LM^3 + LL_xL_y(8M^3 - 4M^2K + 8M^2 + 8M + 14))$

only contains the x coordinates and the y coordinates. The weight calculation does not need complex multiplication. The complexity of different algorithms is given in Table 1.

The computational complexity of the algorithms in Table 1 is shown in Figure 2 when L_x, L_y, L_θ, and L_φ take the same value and change from 1000 to 9000, $K = 3$, $L = 5$, $T = 200$, $M = 10$.

It can be seen from Figure 2 that the proposed NRD-WSDF algorithm has higher computational complexity than the SDF algorithm and the two-step technology. However, since the search dimension of NC phase is removed, the complexity of the proposed NRD-WSDF method is significantly reduced compared with the NC-SDF technology and the NC-WSDF method.

4.2. Simulation and Discussion. We applied Monte Carlo experiments to verify the estimation performance of the proposed NRD-WSDF algorithm. The estimation performance of this algorithm is checked by root mean square error (RMSE) as

$$\mathrm{RMSE} = \frac{1}{K}\sum_{k=1}^{K}\sqrt{\frac{1}{\mathrm{Mon}}\sum_{mn=1}^{\mathrm{Mon}}\left[\left(\hat{x}_{k,mn} - x_k\right)^2 + \left(\hat{y}_{k,mn} - y_k\right)^2\right]}, \tag{43}$$

where K denotes the number of targets, and Mon represents the number of Monte Carlo experiments. All the simulation parameters are given in Table 2. Besides, to express the heteroscedasticity of the observation station conveniently, we define

$$\sigma^2_{\mathrm{error}} = \frac{1}{L}\sum_{l=1}^{L}\left\|\boldsymbol{\alpha}_l - \overline{\alpha}_l\right\|^2, \tag{44}$$

where

$$\begin{aligned}
\boldsymbol{\alpha}_l &= \left[\alpha_{l,1}, \alpha_{l,2}, \ldots, \alpha_{l,K}\right]^T \in \mathbb{R}^{K\times 1},\\
\overline{\alpha}_l &= \left[\overline{\alpha}_l, \overline{\alpha}_l, \ldots, \overline{\alpha}_l\right]^T \in \mathbb{R}^{K\times 1},\\
\overline{\alpha}_l &= \frac{1}{K}\sum_{k=1}^{K}\alpha_{l,k}.
\end{aligned} \tag{45}$$

Simulation 1. This section simulates the proposed algorithm in the underdetermined condition with different SNRs. There are 5 targets incident on the observation stations ($M = 4$, $\sigma^2_{error} = 10$ $T = 200$). The SNRs in Figure 3 and 4 are 0 dB and 20 dB, respectively. From the figures, the proposed NRD-WSDF algorithm can estimate the targets successfully at low SNR and the estimation performance becomes better with the increase of SNR.

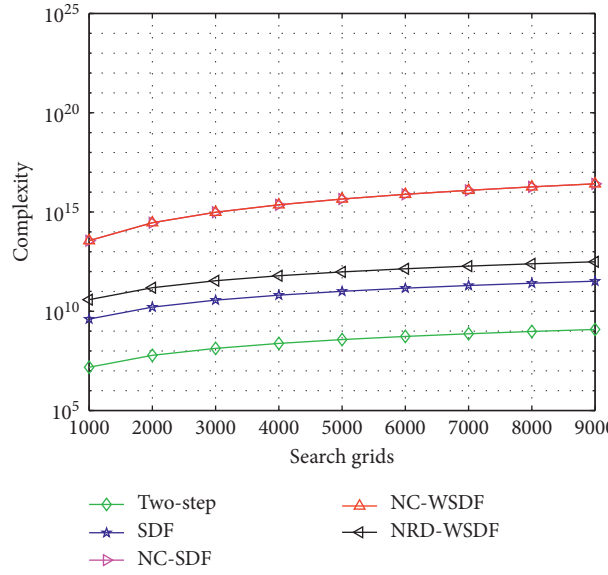

Figure 2: Comparison of different algorithms in complexity.

Simulation 2. This section simulates the proposed algorithm in the underdetermined condition with different snapshots. There are 5 targets incident on the observation stations ($M = 4$, $\sigma^2_{\mathrm{error}} = 10$, SNR = 15 dB). The snapshots in Figure 5 and 6 are 10 and 200, respectively. From the figures, the proposed NRD-WSDF algorithm can estimate the targets successfully with small snapshot, and the estimation accuracy becomes higher with the increase of snapshot.

Simulation 3. Theoretically, the minimum number of array elements M needed to distinguish K targets is $M = (K + 2)/2$. This section simulates the proposed algorithm in the underdetermined condition with different array elements. There are 4 targets incident on the observation stations ($T = 200$, $\sigma^2_{error} = 10$, SNR = 25 dB). Their NC phase and positions are (10, 20, 30, 40) and ((−2900, −2900), (−2900, 2900), (2900, −2900), (2900, 2900)), respectively. The number of array elements in Figures 7 and 8 is 3 and 4, respectively. From the figures, the proposed NRD-WSDF algorithm can estimate the targets successfully with fewer array elements, and the estimation accuracy becomes higher with the increase of array elements.

Table 2: Simulation parameters.

Parameter	Value
M (number of antennas)	4
K (number of targets)	5
T (number of snapshots)	10–500
L (number of observation stations)	6
Mon (number of Monte Carlo)	500
SNR (signal − to − noise ratio)	0–20 dB
σ^2_{error} (heteroscedasticity)	10
$\mathbf{p}$ (target locations)	(−2900, −2900); (−2900, 2900); (0, −1000); (2900, -2900); (2900, 2900)
φ (NC phase)	(10, 20, 30, 40, 50)
$\mathbf{u}$ (observation locations)	(−6000, −9000); (−3600, −7000); (−1200, −10000); (1200, −8000); (3600, −11000); (6000, −12000)

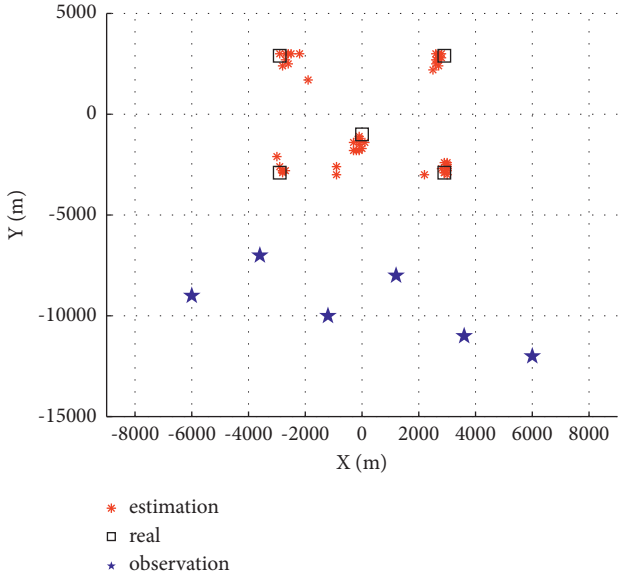

Figure 3: Location performance of NRD-WSDF (SNR = 0 dB).

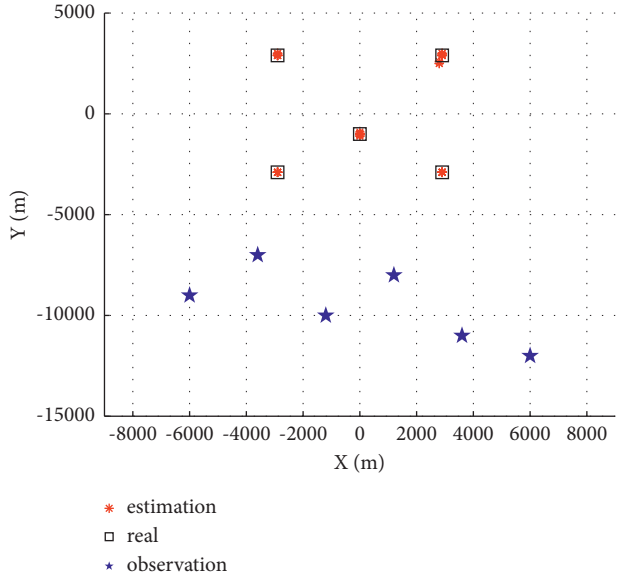

Figure 4: Location performance of NRD-WSDF (SNR = 20 dB).

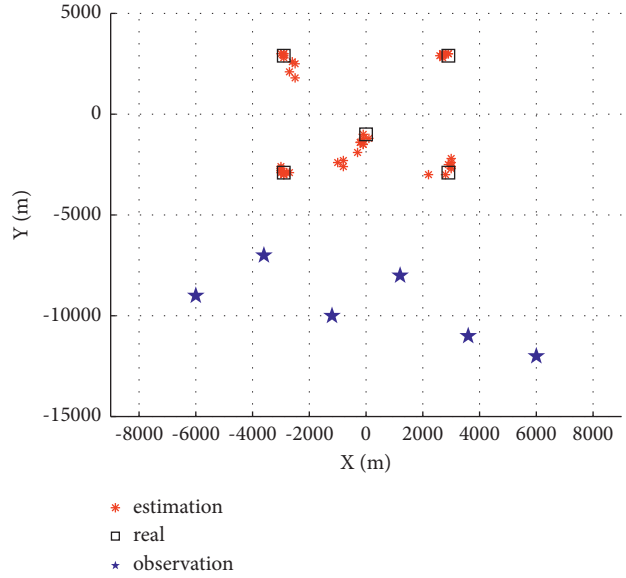

Figure 5: Location performance of NRD-WSDF (snapshot = 10).

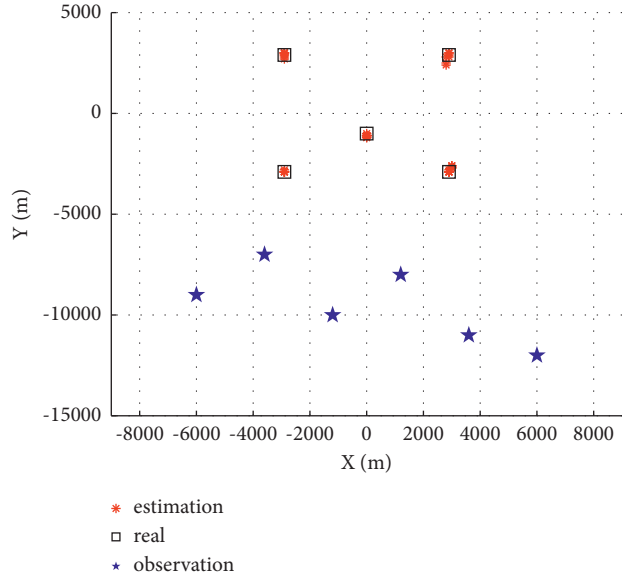

Figure 6: Location performance of NRD-WSDF (snapshot = 200).

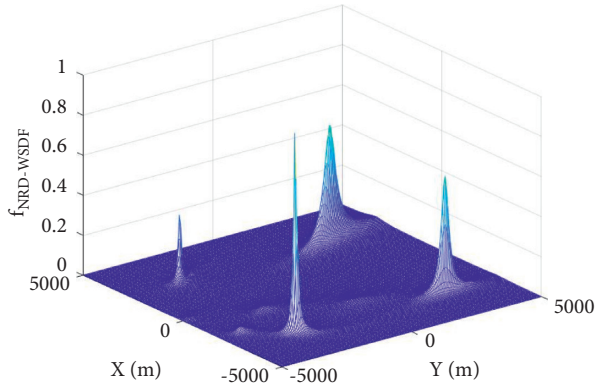

Figure 7: Spectral peak of NRD-WSDF ($M = 3$).

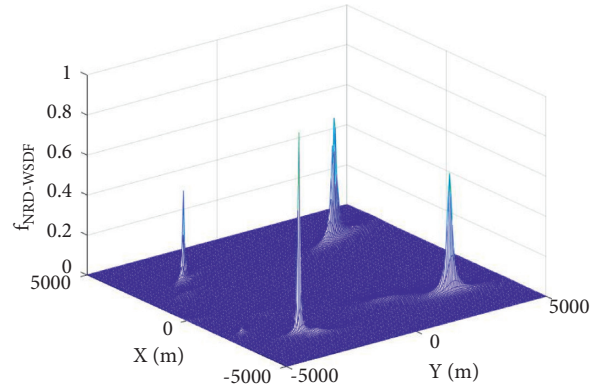

Figure 8: Spectral peak of NRD-WSDF ($M = 4$).

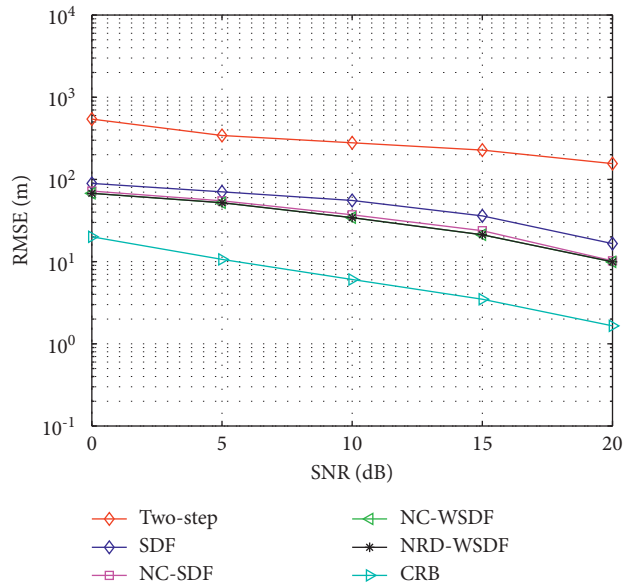

Figure 9: RMSE of different algorithms with different SNRs. (snapshot = 100, $\sigma^2_{error} = 5$).

Simulation 4. This section compares the RMSE performance of different algorithms with different SNRs under different σ^2_{error}. There are 3 targets incident on the observation stations. Their NC phase and positions are (10, 20, 30) and ((−300, −300), (100, 100), (900, 900)), respectively. The other simulation parameters are given in Table 2. The estimation is simulated when σ^2_{error} is 5 (Figure 9) and 50 (Figure 10). The simulation results show that the performance of the proposed NRD-WSDF algorithm is superior than two-step location technology (using ESPRIT technology and clustering algorithm [34]), SDF technology, and NC-SDF method. Compared with the algorithm before dimensionality reduction, the estimation accuracy of the proposed algorithm is close to it. Besides, the excellent performance of

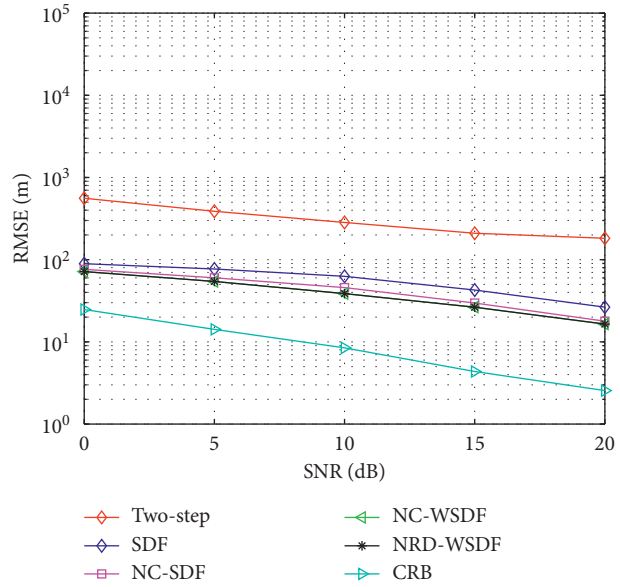

Figure 10: RMSE of different algorithms with different SNRs. (snapshot = 100, $\sigma^2_{error} = 50$).

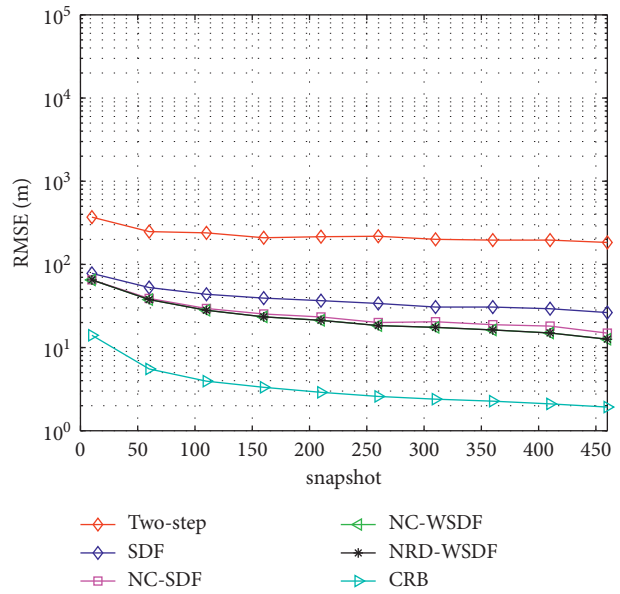

Figure 11: RMSE of different algorithms with different snapshots (SNR = 10 dB, $\sigma^2_{error} = 2$).

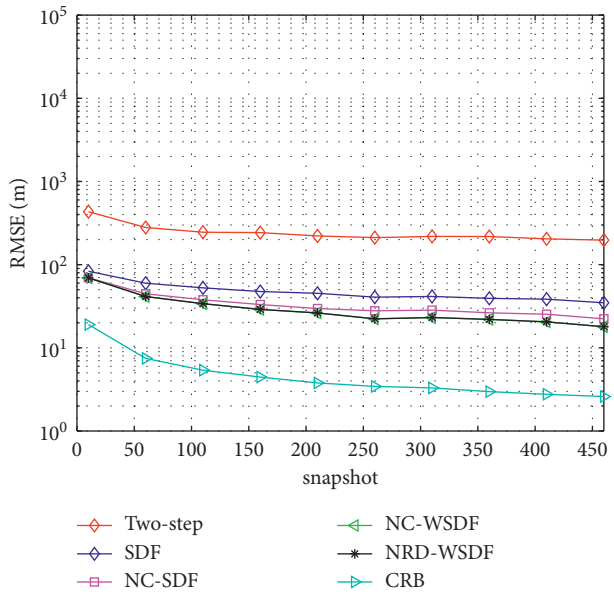

Figure 12: RMSE of different algorithms with different snapshots (SNR = 10 dB, $\sigma^2_{\text{error}} = 50$).

the NRD-WSDF algorithm is more prominent when the heteroscedasticity of observation stations increases.

Simulation 5. This section compares the RMSE performance of different algorithms with different snapshots under different σ^2_{error}. The number of snapshots changed from 10 to 460. The estimation is simulated when σ^2_{error} is 2 (Figure 11) and 50 (Figure 12). The SNR is 10 dB and the other parameters are the same as simulation 3. The simulation results show that the performance of the proposed NRD-WSDF algorithm is better than two-step location technology, SDF method, and NC-SDF technology. Compared with the algorithm before dimensionality reduction, the performance of the proposed algorithm is close to it. Besides, the excellent performance of the NRD-WSDF algorithm is more prominent when the heteroscedasticity of observation stations increases.

5. Conclusions

Existing DPD algorithms of NC signals with multiple arrays do not consider the impact of path propagation loss on the performance of the algorithms, which leads to unstable performance. Thus, we assign a weight to balance the error and obtain higher location accuracy with better robustness. Besides, the high computational complexity caused by NC phase reduces the practicability of the algorithm. So, we introduce the RD method to reduce the computational complexity. The performance analysis confirms that the NRD-WSDF method can effectively improve the location accuracy, get better robustness, and distinguish more targets compared with traditional two-step location technology and SDF technology. In addition, without losing the estimation performance, the proposed algorithm can significantly reduce the complexity caused by the NC phase search dimension.

Data Availability

The data used to support the findings of this study are included within the article.

Conflicts of Interest

The authors declare that they have no conflicts of interest.

Acknowledgments

This work was supported by China NSF (61971217, 61971218, and 61631020), Jiangsu NSF (BK20200444), the funds of Sonar Technology Key Laboratory (Research on the theory and algorithm of signal processing for two-dimensional underwater acoustics coprime array and Range estimation and location technology of passive target via multiple array combination), Jiangsu Key Research and Developement Project (BE2020101), and National Key Research and Development Project (2020YFB1807602).

References

[1] K Hao and Q Wan, "Sparse Bayesian Inference Based Direct Off-Grid Position Determination In Multipath Environments," *IEEE Wireless Communication Letters*, vol. 10, no. 6, pp. 1148–1152, 2021.

[2] J. Su, Z. Yao, and M. Lu, "An improved position determination algorithm based on nonlinear compensation for ground-based positioning systems," *IEEE Access*, vol. 7, pp. 23675–23689, 2019.

[3] S. Mazuelas, R. M. Lorenzo, A. Bahillo, P. Fernandez, J. Prieto, and E. J. Abril, "Topology Assessment Provided by Weighted Barycentric Parameters in Harsh Environment Wireless Location Systems," *IEEE Transactions on Signal Processing*, vol. 58, no. 7, pp. 3842–3857, 2010.

[4] J. K.-Y. Ng, K.-Y. Lam, Q. J. Cheng, and K. C. Y. Shum, "An effective signal strength-based wireless location estimation system for tracking indoor mobile users," *Journal of Computer and System Sciences*, vol. 79, no. 7, pp. 1005–1016, 2013.

[5] Y. L. Wang, Y. Wu, and S. C. Yi, "An efficient direct position determination algorithm combined with time delay and doppler," *Circuits, Systems, and Signal Processing*, vol. 35, no. 2, pp. 635–649, 2016.

[6] S Zhong, X Wei, and Z He, "Adaptive direct position determination of emitters based on time differences of arrival," in *Proceedings of the 2013 IEEE China Summit and International Conference on Signal and Information Processing*, Beijing, China, July 2013.

[7] J. Li, L. Yang, F. Guo, and W. Jiang, "Coherent summation of multiple short-time signals for direct positioning of a wideband source based on delay and Doppler," *Digital Signal Processing*, vol. 48, no. C, pp. 58–70, 2016.

[8] A. Amar and A. J. Weiss, "Direct position determination in the presence of model errors-known waveforms," *Digital Signal Processing*, vol. 16, no. 1, pp. 52–83, 2006.

[9] M. Oispuu and U. Nickel, "Direct detection and position determination of multiple sources with intermittent emission," *Signal Processing*, vol. 90, no. 12, pp. 3056–3064, 2010.

[10] A. J. Weiss, "Direct position determination of narrowband radio frequency transmitters," *IEEE Signal Processing Letters*, vol. 11, no. 5, pp. 513–516, 2004.

[11] B. Picinbono, "On circularity," *IEEE Transactions on Signal Processing*, vol. 42, no. 12, pp. 3473–3482, 1994.

[12] O. Bar-Shalom and A. J. Weiss, "Direct position determination of OFDM signals," in *Proceedings of the IEEE Workshop on Signal Processing Advances in Wireless Communications*, Helsinki, Finland, June 2007.

[13] Z. Shangyu, H. Zhen, F. Xuefeng, H. Jiazhi, and S. Lei, "Multi-sensor passive localization using direct position determination with time-varying delay," *Sensors*, vol. 19, no. 7, Article ID 1541, 2019.

[14] T. Zhou, W. Yi, and L. Kong, "Direct Position Determination of Multiple Coherent Sources Using An Iterative Adaptive Approach," *Signal Processing*, vol. 161, pp. 203–213, 2019.

[15] J.-x. Yin, Y. Wu, and D. Wang, "Direct Position Determination of Multiple Noncircular Sources with a Moving Array," *Circuits, Systems, and Signal Processing*, vol. 36, no. 10, pp. 4050–4076, 2017.

[16] J. Yin, D. Wang, Y. Wu, and X. Yao, "ML-based single-step estimation of the locations of strictly noncircular sources," *Digital Signal Processing*, vol. 69, pp. 224–236, 2017.

[17] J. Yin, D. Wang, and Y. Wu, "An efficient direct position determination method for multiple strictly noncircular sources," *Sensors*, vol. 18, no. 2, Article ID 324, 2018.

[18] Y. K. Zhang, H. Y. Xu, and B. Ba, "Direct position determination of non-circular sources based on a doppler-extended aperture with a moving coprime array," *IEEE Access*, vol. 6, pp. 61014–61021, 2018.

[19] T. Qin, Z. Lu, B. Ba, and D. Wang, "A decoupled direct positioning algorithm for strictly noncircular sources based on doppler shifts and angle of arrival," *IEEE Access*, vol. 6, pp. 34449–34461, 2018.

[20] Y. Zhang, B. Ba, D. Wang, W. Geng, and H. Xu, "Direct position determination of multiple non-circular sources with a moving coprime array," *Sensors*, vol. 18, no. 5, Article ID 1479, 2018.

[21] G. Kumar, P. Ponnusamy, and I. S. Amiri, "Direct localization of multiple noncircular sources with a moving nested array," *IEEE Access*, vol. 7, no. 99, pp. 101106–101116, 2019.

[22] J. Du, H. Yu, D. Wang, and L. Guangyi, "Unified subspace fitting framework and its performance analysis for direct position determination in the presence of multipath propagation," *IEEE Access*, vol. 7, pp. 6889–6914, 2019.

[23] J. Du, D. Wang, W. Yu, and Y. Hongyi, "Direct position determination of unknown signals in the presence of multipath propagation," *Sensors*, vol. 18, no. 3, 2018.

[24] T. Shu, J. He, and L. Li, "Near-field passive localization and gain-phase compensation with partly calibrated arrays," *IEEE Transactions on Aerospace and Electronic Systems*, p. 1, 2021.

[25] T. Shu, J. He, and V. Dakulagi, "3-D near-field source localization using a spatially spread acoustic vector sensor," *IEEE Transactions on Aerospace and Electronic Systems*, p. 1, 2021.

[26] P. Viswanath, D. N. C. Tse, and V. Anantharam, "Asymptotically optimal water-filling in vector multiple-access channels," *IEEE Transactions on Information Theory*, vol. 47, no. 1, 2001.

[27] X. Zhang, J. Li, and D. Xu, *Array signal processing and MATLAB realization*, pp. 181–186, Publishing House of Electronics Industry, Beijing, China, 2020.

[28] X. Zhang, H. Zeng, Z. Wang, and J. Li, "Direct location algorithm of non-circular signals in multiple arrays with the help of dimension reduction search and subspace data fusion," *Data acquisition and processing*, vol. 164, no. 06, pp. 16–26, 2020.

[29] P. Petrus and R. B. Ertel, "Capacity enhancement using adaptive arrays in an AMPS system," *IEEE Transactions on Vehicular Technology*, vol. 47, no. 3, 1998.

[30] S.-S. Jeng, H.-P. Lin, and W. J. Vogel, "Experimental studies of spatial signature variation at 900 MHz forsmart antenna systems," *IEEE Transactions on Antennas & Propagation*, vol. 46, no. 7, 1998.

[31] Y. Qian, Z. Yang, and H. Zeng, "Direct position determination for augmented coprime arrays via weighted subspace data fusion method," *Mathematical Problems in Engineering*, vol. 2021, no. 3, pp. 1–10, 2021.

[32] X. Zhang, L. Xu, L. Xu, and D. Xu, "Direction of departure (DOD) and direction of arrival (DOA) estimation in MIMO radar with reduced-dimension music," *IEEE communications letters*, vol. 14, no. 12, pp. 1161–1163, 2010.

[33] X. Zhang and D. Xu, "Angle estimation in bistatic MIMO radar using improved reduced dimension Capon algorithm," *Journal of Systems Engineering and Electronics*, vol. 24, no. 1, pp. 84–89, 2013.

[34] J. Jun Liu, J. P. Y. Lee, L. Lingjie Li, Z.-Q. Zhi-Quan Luo, and K. M. Wong, "Online clustering algorithms for radar emitter classification," *IEEE Transactions on Pattern Analysis and Machine Intelligence*, vol. 27, no. 8, pp. 1185–1196, 2005.